



Synthesis and Antiprotozoal Evaluation of New 2,9-bis[(pyridinylalkylaminomethyl)phenyl]-1,10-Phenanthroline Derivatives by Targeting G-quadruplex, an Interesting Pharmacophore Against Drug Efflux

Jean Guillon^{1*}, Anita Cohen², Sarah Monic^{1,3}, Clotilde Boudot⁴, Solène Savrimoutou¹, Sandra Albenque-Rubio¹, Stéphane Moreau¹, Alexandra Dassonville-Klimpt⁵, Jean-Louis Mergny⁶, Luisa Ronga⁷, Mikel Bernabeu de Maria⁷, Nikita Tyurin-Schmitt¹, Paul Parrens¹, Adrien Labarthe¹, Valentin Gomez¹, Serge Moukha^{8,9}, Pascale Dozolme^{8,9}, Nadine Azas², Valérie Gabelica¹⁰, Patrice Agnamey⁵, Céline Damiani^{5,11}, Anne Totet^{5,11}, Catherine Mullié⁵, Bertrand Courtioux⁴ and Pascal Sonnet⁵

¹University of Bordeaux, Faculty of Pharmacy, CNRS, INSERM, ARNA, UMR 5320, U1212, France

²University of Aix-Marseille, IRD, AP-HM, SSA, VITROME, Marseille, France

³Department of Biochemistry, University of Cambridge, Tennis Court Road, Cambridge CB2 1QW, United Kingdom

⁴University of Limoges, INSERM U1094, Tropical Neuroepidemiology, Limoges, France and Institute of Neuroepidemiology and Tropical Neurology, France

⁵University of Picardie Jules Verne, Agents Infectieux, Résistance et Chimiothérapie (AGIR), UR 4294, UFR de Pharmacie, France

⁶Ecole Polytechnique, Laboratoire d'Optique et Biosciences, CNRS, INSERM, Institut Polytechnique de Paris, France

⁷Université de Pau et des Pays de l'Adour, E2S UPPA, CNRS, IPREM, France

⁸Centre de Recherche Cardio-thoracique de Bordeaux (CRCTB), UMR U1045 INSERM, PTIB - Hôpital Xavier Arnoz, France

⁹INRAE Bordeaux Aquitaine, F- 33140 Villenave-d'Ornon, France

¹⁰University of Bordeaux, IECB, CNRS, INSERM, ARNA, France

¹¹Laboratoire de Parasitologie-Mycologie, Centre de Biologie Humaine, CHU Amiens-Picardie, France

*Corresponding Author: Jean Guillon, University of Bordeaux, Faculty of Pharmacy, CNRS, INSERM, ARNA, UMR 5320, U1212, France.

DOI: 10.31080/ASPS.2023.07.0934

Abstract

A series of new 2,9-bis[(pyridinylalkylaminomethyl)phenyl]-1,10-phenanthroline compounds was considered, synthesized, and evaluated *in vitro* against three parasites (*Plasmodium falciparum*, *Leishmania donovani* and *Trypanosoma brucei brucei*). Pharmacological results showed antiparasitic activity with IC₅₀ values in the sub and μM range. The *in vitro* cytotoxicity of these novel aza derivatives was evaluated on human HepG2 cells. The phenanthroline 1f was noticed as the most potent antimalarial candidate with a ratio of cytotoxic to antiprotozoal activities of 912.4 against the *P. falciparum* CQ-resistant strain W2. In addition, the phenanthroline 1a was also identified as the most potent antiparasitic derivative with a selectivity index (SI) of 811.8 on *P. falciparum* CQ-sensitive strain 3D7. Against the promastigote forms of *L. donovani*, the same phenanthroline 1a was found the most active compounds with an IC₅₀ of 2.08 mM. In addition, the phenanthrolines 1f and 1i were also identified as the most promising trypanosomal candidates with selectivity index (SI) of 231.1 and 143.7, respectively on *T. brucei brucei* strain. As the telomeres of the parasites *P. falciparum* and *Trypanosoma* could be considered as possible targets of this kind of aza heterocyclic molecules, their ability to stabilize the parasitic telomeric G-quadruplexes have been measured through the FRET melting assay.

Keywords: Phenanthroline; G-quadruplex; Antimalarial Activity; Antileishmanial Activity; Antitrypanosomal Activity

Introduction

Malaria control is worldwide impacted by a host of challenges, including the long-running COVID-19 crisis, the potential effect of climate change and the decline in the effectiveness of the existing fighting tools. To date, there were an estimated 247 million malaria cases in 2021 in 84 malaria endemic countries, an increase from 2020 (245 million) with most of this increase in the WHO African region. Globally, malaria deaths amounted to 619 000 in 2021, with 63 000 deaths between 2019 and 2021 due to disruptions to essential malaria services during the COVID-19 pandemic [1]. Four countries in the WHO African Region (Nigeria, the Democratic Republic of the Congo, the United Republic of Tanzania and Niger) represented just over half of all malaria deaths in 2021 [1]. In these conditions, the WHO regularly published most up to date guidelines which encourage countries to adapt the recommendations to local settings [2]. In Africa in particular, an initiative to stop the spread of the *Anopheles stephensi* mosquito, which is adapted to urban environments and resistant to several insecticides, and a response strategy to the worrying resistance to antimalarial drugs were necessary. Indeed, a worrying *de novo* emergence of artemisinin partial resistance in this region led the WHO, in November 2022, to launch a specific strategy to respond to the urgent problem of antimalarial drug resistance in Africa, such as Artemisinin-based combination therapy (ACT) is the mainstay of malaria care [3]. WHO has also developed a series of tools to facilitate the work of national malaria programs and other partners involved in routine testing of antimalarial drug efficacy [4]. Furthermore, it appears urgent to implement vigorous measures to protect the effectiveness of existing antimalarial drugs and to develop new drug candidates with novel targets [5]. In this context, efflux mechanism has long appeared as a potential and attractive target to combat multidrug resistant *Plasmodium falciparum* [6,7] and efforts to discover in particular new 4-aminoquinoline derivatives are ongoing. Indeed, it is unlikely that the parasite will be able to evolve resistance to drugs targeting the pathway involved in hemoglobin degradation. Previous studies have shown that modification and modulation of the lateral side chain of chloroquine (CQ) or of mefloquine (MQ) that led to original aminoquinoline derivatives could avoid the chloroquine resistance mechanism [8-11]. Another developed strategy is to design and synthesize quinoline-based drugs that could not be recognized by the protein system involved in the drug

efflux. The efflux pumps serve both as natural defense mechanisms and influence the bioavailability and disposition of drugs. Initially, such mechanism was suggested in *Plasmodium falciparum* where erythrocytes infected with chloroquine resistant parasites accumulated significantly less drug than the sensitive ones [12], before its further study led to the identification of the *Pfcr* gene [13] among other quinoline drug resistance mechanisms [14]. Consequently new series not recognized by the protein system involved in the drug efflux of bisquinoline and bisacridine antimalarial drugs (Figure 1, A, B and Piperaquine) have been previously described in the literature [10,15-17]. These new nitrogen molecules had much lower resistance indices than CQ, indicating that these heterocyclic derivatives are less efficiently rejected by efflux by drug-resistant parasites. In addition, previous studies on *in vitro* antiplasmodial activity of dinitrogen phenanthrene homologs indicated that the 1,10-phenanthroline skeleton represents a potential antimalarial lead compound. Some bioactive antiprotozoal phenanthrolines based on this structure have been described such as 4,7-phenanthrolines C and D (Figure 1) [18], 4-chloro-2-methyl-3-vinyl-1,10-phenanthroline E (Figure 1) [19], 4-methoxy-11-methyl-3*H*-pyrrolo[3,2-*c*] [1,10]phenanthroline F (Figure 1) [20], and *N*-benzyl-1,10-phenanthroline iodide G (Figure 1) [21,22]. This phenanthroline moiety could also be considered as a bioisoster of the phenanthrene heterocycle found in the halofantrine's structure [5]. Moreover, the study of the trypanocidal activity of new anilinophenanthroline derivatives H-J against *Trypanosoma cruzi* has also been described [23].

Nevertheless, among the protozoa of medical interest, trypanosomatid parasites are also important, responsible for tropical diseases, mainly leishmaniasis caused by more than 20 *Leishmania* species described to be infective to humans, and trypanosomiasis including human African trypanosomiasis (or sleeping sickness) caused by *Trypanosoma brucei* and South American trypanosomiasis (or Chagas disease) caused by *Trypanosoma cruzi*. Considered as neglected tropical diseases according to the WHO, that wants to eliminate them as a public health problem by 2030 [24], their impact is even more important because of the current limited therapeutic arsenal which is highly toxic and subject to the development of increasingly drug-resistant parasite strains [25].

During our research focused on the discovery of new aza heterocyclic derivatives for use in anticancer chemotherapy, we prepared a series of substituted 2,9-bis[(pyridinylalkylaminomethyl)phenyl]-1,10-phenanthroline derivatives 1 (Figure 1, Series B) designed to bind to DNA G-quadruplexes [26]. As these 2,9-bis[(pyridinylalkylaminomethyl)phenyl]-1,10-phenanthrolines possess the structural parameters required for an antimalarial activity, we decided to enlarge these series and synthesize new substituted 1,10-phenanthroline compounds 1 (Figure 1) taking into account our experience in the field of the synthesis of new antiprotozoal heterocyclic compounds [27-32]. Moreover, these phenanthroline

1 could be also considered as new bioisosters of the previously synthesized series A (Figure 1) which have showed promising antiprotozoal results by our team [33].

We report on their *in vitro* antiplasmodial activity against the chloroquine-sensitive (3D7) and the chloroquine-resistant (W2) strains of the malaria parasite *P.falciparum*. As nitrogen heterocyclic scaffolds are the fundamental units of many antiprotozoan candidates, these quinoline-like derivatives were also tested for *in vitro* efficacy against medically important protozoans *Leishmania donovani* and *Trypanosoma brucei brucei*.

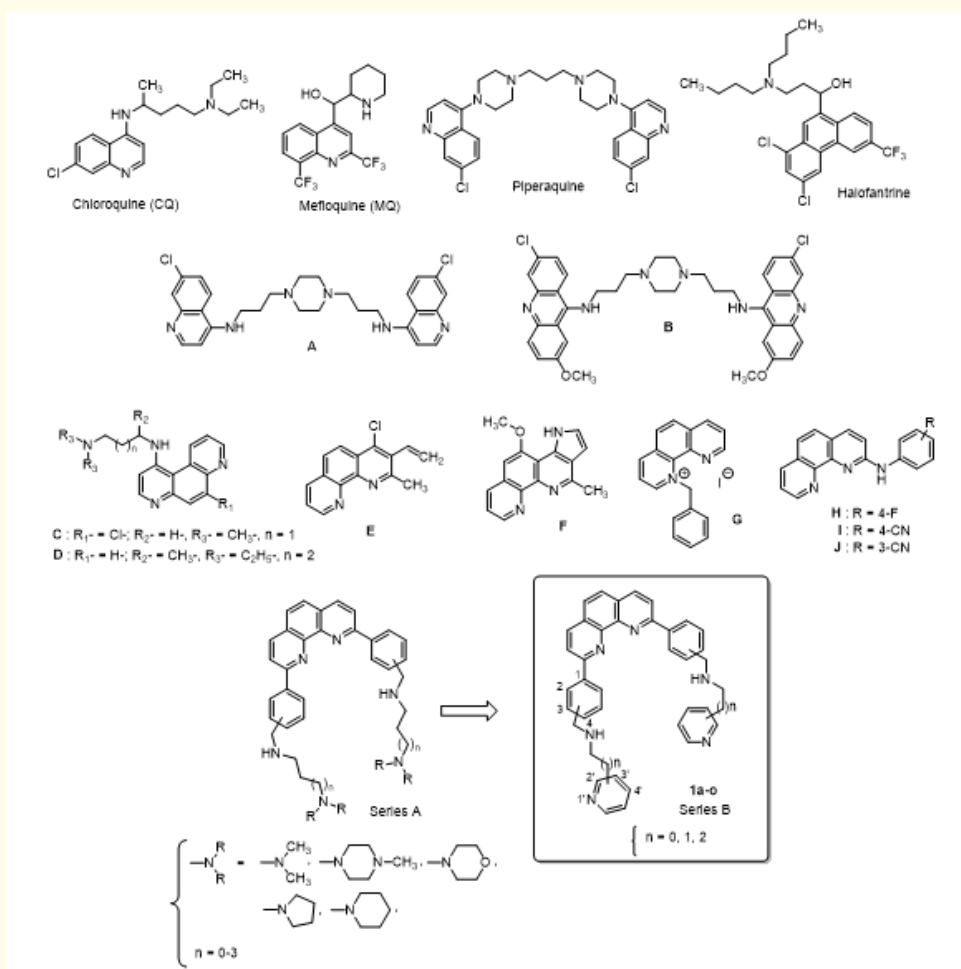


Figure 1: Chemical structures of chloroquine, mefloquine, piperaquine, halofantrine, bisquinoline A, bisacridine B, 4,7-phenanthrolines C and D, 4-chloro-2-methyl-3-vinyl-1,10-phenanthroline E, 4-methoxy-11-methyl-3H-pyrrolo[3,2-c][1,10]phenanthroline F, N-benzyl-1,10-phenanthroline G, anilino-phenanthrolines H-J and newly synthesized substituted phenanthroline derivatives 1a-o.

In addition, the *in vitro* cytotoxicity of our new 2,9-bis[(pyridinylalkylaminomethyl)phenyl]-1,10-phenanthroline derivatives 1 was assessed in human HepG2 cells, and an index of selectivity, the ratio of cytotoxic to antiparasitic activity, was determined for each derivative. The telomeres of the different protozoa could constitute attractive drug targets [34-37] in order to bypass the resistance mechanisms based on efflux and telomerase activity is detected in gametocytes and during the transition to the erythrocytic stage of *P. falciparum* [38]. The telomeric 3' G-overhang region of *P. falciparum* is a repetition of degenerate unit 5'GGGTTA3' (where Y could be T or C) [39] which can fold into intramolecular G-quadruplex [39]. This difference between parasitic and human (5'GGGTTA3') G-quadruplexes is also observed with *L. spp* and *T. brucei brucei*, which augurs the possibility of developing antiparasitic ligands targeting specifically G-quadruplexes found in these protozoal species. Thus, we investigated whether the most promising bioactive derivatives could stabilize some parasitic telomeric DNA G-quadruplex structures. Consequently, potential stabilization of *P. falciparum* and *T. brucei brucei* telomeric G-quadruplexes was evaluated using a FRET melting assay.

Materials and Methods

Chemistry

Commercially available reagents were used as received without additional purification. Melting points were determined with an SM-LUX-POL Leitz hot-stage microscope (Leitz GMBH, Midland, ON, USA) and are uncorrected. NMR spectra were recorded with tetramethylsilane as an internal standard using a BRUKER AVANCE 300 spectrometer (Bruker BioSpin, Wissembourg, France). Splitting patterns have been reported as follows: s = singlet; bs = broad singlet; d = doublet; t = triplet; q = quartet; dd = double doublet; ddd = double double doublet; qt = quintuplet; m = multiplet. Analytical TLC were carried out on 0.25 precoated silica gel plates (POLYGRAM SIL G/UV254) and visualization of compounds after UV light irradiation. Silica gel 60 (70-230 mesh) was used for column chromatography. Mass spectra were recorded on an ESI LTQ Orbitrap Velos mass spectrometer (ThermoFisher, Bremen, Germany). Elemental analyses were found within $\pm 0.4\%$ of the theoretical values. Phenanthrolines 1a-i were synthesized as previously described in reference [26].

General procedure for the synthesis of 2,9-bis[2- or 3-(pyridinylalkyliminomethyl)phenyl]-1,10-phenanthrolines 3j-o

The bis-[2,9-(formylphenyl)]-1,10-phenanthroline **2** (150 mg, 0.386 mmol) was dissolved in 6 mL of toluene. Activated molecular sieves 4 Å (800 mg) were introduced and then pyridinylalkylamine (0.812 mmol). The reaction mixture was stirred in a stoppered flask 24 hours. The suspension that was obtained was filtered, washed with dichloromethane, then the solvent was removed under reduced pressure to afford the di-imine **3**.

2,9-Bis[2-(pyridin-4-ylmethyliminomethyl)phenyl]-1,10-phenanthroline (3j)

Yellow crystal (yield, 70%), mp = 104°C. ¹H NMR (CDCl₃) δ ppm: 9.14 (s, 2H, 2 CH=N), 8.41 (dd, 4H, J = 6.00 and 1.50 Hz, 2 H-2_{pyr}, 2 H-6_{pyr}), 8.36 (d, 2H, J = 8.40 Hz, H-4 and H-7), 8.24 - 8.20 (m, 2H, 2 H-6'), 7.92 (d, 2H, J = 8.40 Hz, H-3 and H-8), 7.90 (s, 2H, H-5 and H-6), 7.84-7.80 (m, 2H, 2 H-3'), 7.54 - 7.50 (m, 4H, 2 H-4' and 2 H-5'), 7.10 (dd, 4H, J = 6.00 and 1.50 Hz, 2 H-3_{pyr} and 2H-5_{pyr}), 4.56 (s, 4H, 2 NCH₂).

2,9-Bis[2-(pyridin-4-ylethyliminomethyl)phenyl]-1,10-phenanthroline (3k)

Orange oil (yield, 84%). ¹H NMR (CDCl₃) δ ppm: 8.74 (s, 2H, 2 CH=N), 8.35 (dd, 4H, J = 5.90 and 1.50 Hz, 2 H-2_{pyr}, 2 H-6_{pyr}), 8.26 (d, 2H, J = 8.40 Hz, H-4 and H-7), 8.09 - 8.04 (m, 2H, 2 H-6'), 7.87 (s, 2H, H-5 and H-6), 7.74-7.71 (m, 2H, 2 H-3'), 7.63 (d, 2H, J = 8.40 Hz, H-3 and H-8), 7.47 - 7.42 (m, 4H, 2 H-4' and 2 H-5'), 6.89 (dd, 4H, J = 6.00 and 1.50 Hz, 2 H-3_{pyr} and 2H-5_{pyr}), 3.61 (t, 4H, J = 7.20 Hz, 2 NCH₂), 2.83 (t, 4H, J = 7.20 Hz, 2 CH_{2pyr}).

2,9-Bis[2-(pyridin-4-ylpropyliminomethyl)phenyl]-1,10-phenanthroline (3l)

Yellow oil (yield, 87%). ¹H NMR (CDCl₃) δ ppm: 8.87 (s, 2H, 2 CH=N), 8.35 (dd, 4H, J = 6.00 and 1.50 Hz, 2 H-2_{pyr}, 2 H-6_{pyr}), 8.34 (d, 2H, J = 8.10 Hz, H-4 and H-7), 8.15 - 8.11 (m, 2H, 2 H-6'), 7.90 (s, 2H, H-5 and H-6), 7.83 (d, 2H, J = 8.10 Hz, H-3 and H-8), 7.78-7.75 (m, 2H, 2 H-3'), 7.52 - 7.45 (m, 4H, 2 H-4' and 2 H-5'), 6.97 (dd, 4H, J = 6.00 and 1.50 Hz, 2 H-3_{pyr} and 2H-5_{pyr}), 3.46 (t, 4H, J = 6.90 Hz, 2 NCH₂), 2.51 (t, 4H, J = 6.90 Hz, 2 NCH_{2pyr}), 1.91 (qt, 4H, J = 6.90 Hz, 2 CH₂).

2,9-Bis[3-(pyridin-4-ylmethyliminomethyl)phenyl]-1,10-phenanthroline (3m)

Yellow orange oil (yield, 75%). ¹H NMR (CDCl₃) δ ppm: 8.81 (d, 2H, J = 1.20 Hz, 2 H-2'), 8.71 (dd, 2H, J = 7.50 and 1.20 Hz, 2 H-6'), 8.61 – 8.57 (m, 6H, 2 H-2_{pyr}, 2 H-6_{pyr} and 2 CH=N), 8.36 (d, 2H, J = 8.40 Hz, H-4 and H-7), 8.24 (d, 2H, J = 8.40 Hz, H-3 and H-8), 7.94 (dd, 2H, J = 7.50 and 1.20 Hz, 2 H-4'), 7.84 (s, 2H, H-5 and H-6), 7.64 (t, 2H, J = 7.50 Hz, 2 H-5'), 7.34 (dd, 4H, J = 6.00 and 1.50 Hz, 2 H-3_{pyr} and 2H-5_{pyr}), 4.75 (s, 4H, 2 NCH₂_{pyr}).

2,9-Bis[3-(pyridin-4-ylethyliminomethyl)phenyl]-1,10-phenanthroline (3n)

Pale yellow crystals (yield, 81%), mp = 181°C. ¹H NMR (CDCl₃) δ ppm: 8.70-8.66 (m, 4H, 2H-2' and 2 H-6'), 8.52 (dd, 4H, J = 6.00 and 1.50 Hz, 2 H-2_{pyr} and 2 H-6_{pyr}), 8.33 (s, 2H, 2 CH=N), 8.32 (d, 2H, J = 8.40 Hz, H-4 and H-7), 8.20 (d, 2H, J = 8.40 Hz, H-3 and H-8), 7.84 (dd, 2H, J = 7.50 and 1.20 Hz, 2 H-4'), 7.80 (s, 2H, H-5 and H-6), 7.65 (t, 2H, J = 7.50 Hz, 2 H-5'), 7.20 (dd, 4H, J = 6.00 and 1.50 Hz, 2 H-3_{pyr} and 2 H-5_{pyr}), 3.93 (t, 4H, J = 7.20 Hz, 2 NCH₂_{pyr}), 3.06 (t, 4H, J = 7.20 Hz, 2 CH₂_{pyr}).

2,9-Bis[3-(pyridin-4-ylpropyliminomethyl)phenyl]-1,10-phenanthroline (3o)

Yellow oil (yield, 96%). ¹H NMR (CDCl₃) δ ppm: 8.73 (d, 2H, J = 1.20 Hz, 2 H-2'), 8.72-8.68 (m, 2H, 2 H-6'), 8.52 (dd, 4H, J = 6.00 and 1.50 Hz, 2 H-2_{pyr} and 2H-6_{pyr}), 8.47 (s, 2H, 2 CH=N), 8.37 (d, 2H, J = 8.40 Hz, H-4 and H-7), 8.26 (d, 2H, J = 8.40 Hz, H-3 and H-8), 7.89 (dd, 2H, J = 7.50 and 1.20 Hz, 2 H-4'), 7.85 (s, 2H, H-5 and H-6), 7.67 (t, 2H, J = 7.80 Hz, 2 H-5'), 7.20 (dd, 4H, J = 6.00 and 1.20 Hz, 2 H-3_{pyr} and 2 H-5_{pyr}), 3.73 (t, 4H, J = 6.90 Hz, 2 NCH₂_{pyr}), 2.77 (t, 4H, J = 7.20 Hz, 2 CH₂_{pyr}), 2.13 (qt, 4H, J = 6.90 Hz, 2 CH₂).

General procedure for the synthesis of 2,9-bis[2-or3-(pyridinylalkylaminomethyl)phenyl]-1,10-phenanthrolines 1j-o

To a solution of compound 3j-o (0.4 mmol) in methanol (10 mL) was added portion-wise at 0°C sodium borohydride (2.4 mmol, 6 eq.). The reaction mixture was then stirred at room temperature for 2 hours. Then it was evaporated to dryness under reduced pressure. After cooling, the residue was triturated in water and extracted with dichloromethane (40 ml). The organic layer was separated, dried over sodium sulfate and activated charcoal and

evaporated to dryness. The residue was then purified by column chromatography on silica gel using dichloromethane/methanol (90/10: v/v) as eluent to give the pure products 1j-o.

2,9-Bis[2-(pyridin-4-ylmethylaminomethyl)phenyl]-1,10-phenanthroline (1j)

Yellow-crystals (yield, 93%), mp = 73°C. ¹H NMR (CDCl₃) δ ppm: 8.38 (d, 2H, J = 8.40 Hz, H-4 and H-7), 8.24 (dd, 4H, J = 6.00 and 1.50 Hz, 2 H-2_{pyr} and 2 H-6_{pyr}), 7.93 (s, 2H, H-5 and H-6), 7.87 (d, 2H, J = 8.40 Hz, H-3 and H-8), 7.59 – 7.53 (m, 2H, 2 H-6'), 7.37 – 7.26 (m, 6H, 2 H-3', 2 H-4', 2 H-5'), 7.00 (dd, 4H, J = 6.00 and 1.50 Hz, 2 H-3_{pyr} and 2 H-5_{pyr}), 3.59 (s, 4H, 2 NCH₂), 3.48 (s, 4H, 2 NCH₂_{pyr}); ¹³C NMR (CDCl₃) δ ppm: 160.9 (C-2 and C-9), 150.8 (C-4_{pyr}), 150.6 (C-2_{pyr} and C-6_{pyr}), 146.6 (C-1a and C-10a), 142.4 (C-1' and C-2'), 138.2 (C-4 and C-7), 132.9 (C-3'), 131.5 (C-5'), 130.1 (C-4'), 129.3 (C-4a and C-6a), 128.7 (C-6'), 127.7 (C-5 and C-6), 125.0 (C-3 and C-8), 124.5 (C-3_{pyr} and C-5_{pyr}), 52.6 (2 NCH₂); ESI-MS m/z [M+H]⁺ Calcd for C₃₈H₃₃N₆: 573.2767, Found: 573.2755.

2,9-Bis[2-(pyridin-4-ylethylaminomethyl)phenyl]-1,10-phenanthroline (1k)

Yellow-oil (yield, 92%). ¹H NMR (CDCl₃) δ ppm: 8.37 (d, 2H, J = 8.40 Hz, H-4 and H-7), 8.31 (dd, 4H, J = 6.00 and 1.50 Hz, 2 H-2_{pyr} and 2 H-6_{pyr}), 7.91 (s, 2H, H-5 and H-6), 7.83 (d, 2H, J = 8.40 Hz, H-3 and H-8), 7.51 – 7.42 (m, 4H, 2 H-6' and 2 H-3'), 7.33 – 7.28 (m, 4H, 2 H-4' and 2 H-5'), 6.72 (dd, 4H, J = 6.00 and 1.50 Hz, 2 H-3_{pyr} and 2 H-5_{pyr}), 3.61 (s, 4H, 2 NCH₂), 2.59 (t, 4H, J = 7.50 Hz, 2 NH₂), 2.26 (t, 4H, J = 7.50 Hz, 2 CH₂_{pyr}); ¹³C NMR (CDCl₃) δ ppm: 161.0 (C-2 and C-9), 150.8 (C-4_{pyr}), 150.6 (C-2_{pyr} and C-6_{pyr}), 146.5 (C-1a and C-10a), 142.7 (C-1' and C-2'), 138.3 (C-4 and C-7), 133.2 (C-3'), 131.3 (C-5'), 130.1 (C-4'), 129.4 (C-4a and C-6a), 128.8 (C-6'), 127.8 (C-5 and C-6), 125.5 (C-3_{pyr} and C-5_{pyr}), 125.1 (C-3 and C-8), 52.7 (NCH₂), 50.6 (NCH₂), 36.1 (CH₂_{pyr}); ESI-MS m/z [M+H]⁺ Calcd for C₄₀H₃₇N₆: 601.3080, Found: 601.3070.

2,9-Bis[2-(pyridin-4-ylpropylaminomethyl)phenyl]-1,10-phenanthroline (1l)

Yellow-oil (yield, 98%). ¹H NMR (CDCl₃) δ ppm: 8.40 (d, 2H, J = 8.40 Hz, H-4 and H-7), 8.34 (dd, 4H, J = 6.00 and 1.20 Hz, 2 H-2_{pyr} and 2 H-6_{pyr}), 7.91 (s, 2H, H-5 and H-6), 7.88 (d, 2H, J = 8.40 Hz, H-3 and H-8), 7.58 – 7.52 (m, 4H, 2 H-6' and 2 H-3'), 7.40 – 7.35 (m, 4H, 2 H-4' and 2 H-5'), 6.79 (dd, 4H, J = 6.00 and 1.20 Hz, 2 H-3_{pyr} and 2

H-5_{pyr}), 3.73 (s, 4H, 2 NCH₂), 2.47 (t, 4H, J = 6.90 Hz, 2 NH₂), 2.25 (t, 4H, J = 6.90 Hz, 2 CH_{2pyr}), 1.37 (qt, 4H, J = 6.90 Hz, 2 CH₂); ESI-MS m/z [M+H]⁺ Calcd for C₄₂H₄₁N₆: 629.3393, Found: 629.3379.

2,9-Bis[3-(pyridin-4-ylmethylaminomethyl)phenyl]-1,10-phenanthroline (1m)

Yellow-orange oil (yield, 90%). ¹H NMR (CDCl₃) δ ppm: 8.55 (dd, 4H, J = 6.00 and 1.50 Hz, 2 H-2_{pyr} and 2 H-6_{pyr}), 8.54 (d, 2H, J = 1.20 Hz, 2 H-2'), 8.37 (d, 2H, J = 8.40 Hz, H-4 and H-7), 8.36 (dd, 2H, J = 7.50 and 1.20 Hz, 2 H-6'), 8.19 (d, 2H, J = 8.40 Hz, H-3 and H-8), 7.84 (s, 2H, H-5 and H-6), 7.54 (t, 2H, J = 7.50 Hz, 2 H-5'), 7.46 (dd, 2H, J = 7.50 and 1.20 Hz, 2 H-4'), 7.35 (dd, 4H, J = 6.00 and 1.50 Hz, 2 H-3_{pyr} and 2 H-5_{pyr}), 4.02 (s, 4H, 2 NCH₂), 3.91 (s, 4H, 2 NCH_{2pyr}); ¹³C NMR (CDCl₃) δ ppm: 158.1 (C-2 and C-9), 151.2 (C-2_{pyr} and C-6_{pyr}), 150.5 (C-4_{pyr}), 147.4 (C-1a and C-10a), 141.4 (C-3'), 141.1 (C-1'), 138.4 (C-4 and C-7), 130.7 (C-2'), 130.4 (C-4'), 129.4 (C-4a and C-6a), 128.9 (C-5'), 128.0 (C-6'), 127.5 (C-5 and C-6), 124.5 (C-3_{pyr} and C-5_{pyr}), 121.6 (C-3 and C-8), 54.7 (NCH₂), 53.0 (NCH_{2pyr}); ESI-MS m/z [M+H]⁺ Calcd for C₃₈H₃₃N₆: 573.2767, Found: 573.2758.

2,9-Bis[3-(pyridin-4-ylethylaminomethyl)phenyl]-1,10-phenanthroline (1n)

Yellow-orange oil (yield, 55%). ¹H NMR (CDCl₃) δ ppm: 8.51 – 8.48 (m, 6H, 2H-2', 2 H-2_{pyr} and 2 H-6_{pyr}), 8.35 (d, 2H, J = 8.40 Hz, H-4 and H-7), 8.31 (dd, 2H, J = 7.50 and 1.20 Hz, 2 H-6'), 8.16 (d, 2H, J = 8.40 Hz, H-3 and H-8), 7.84 (s, 2H, H-5 and H-6), 7.54 (t, 2H, J = 7.50 Hz, 2 H-5'), 7.41 (dd, 2H, J = 7.50 and 1.20 Hz, 2 H-4'), 7.15 (dd, 4H, J = 6.00 and 1.50 Hz, 2 H-3_{pyr} and 2 H-5_{pyr}), 4.12 (s, 4H, 2 NCH₂), 3.00 (t, 4H, J = 6.90 Hz, 2 NCH₂), 2.98 (t, 4H, J = 6.90 Hz, 2 CH_{2pyr}); ESI-MS m/z [M+H]⁺ Calcd for C₄₀H₃₇N₆: 601.3079, Found: 601.3071.

2,9-Bis[3-(pyridin-4-ylpropylaminomethyl)phenyl]-1,10-phenanthroline (1o)

Yellow oil (yield, 97%). ¹H NMR (CDCl₃) δ ppm: 8.44-8.40 (m, 6H, 2H-2', 2 H-2_{pyr} and 2 H-6_{pyr}), 8.34 (dd, 2H, J = 7.80 and 1.50 Hz, 2 H-6'), 8.28 (d, 2H, J = 8.40 Hz, H-4 and H-7), 8.14 (d, 2H, J = 8.40 Hz, H-3 and H-8), 7.76 (s, 2H, H-5 and H-6), 7.52 (t, 2H, J = 7.80 Hz, 2 H-5'), 7.43 (dd, 2H, J = 7.80 and 1.50 Hz, 2 H-4'), 7.07 (dd, 4H, J = 6.00 and 1.20 Hz, 2 H-3_{pyr} and 2 H-5_{pyr}), 3.95 (s, 4H, 2 NCH₂), 2.71 (t, 4H, J = 6.90 Hz, 2 NCH₂), 2.64 (t, 4H, J = 6.90 Hz, 2 CH_{2pyr}), 1.84 (qt, 4H, J = 6.90 Hz, 2 CH₂); ¹³C NMR (CDCl₃) δ ppm: 158 (C-2 and C-9), 152.5 (C-4_{pyr}), 151.0 (C-2_{pyr} and C-6_{pyr}), 147.4 (C-1a and C-10a),

142.1 (C-3'), 141.0 (C-1'), 138.3 (C-4 and C-7), 130.7 (C-2'), 130.3 (C-4'), 129.3 (C-4a and C-6a), 128.8 (C-5'), 127.8 (C-6'), 127.4 (C-5 and C-6), 125.2 (C-3_{pyr} and C-5_{pyr}), 121.4 (C-3 and C-8), 55.5 (NCH₂), 49.9 (NCH₂), 34.2 (CH₂), 32.0 (CH₂); ESI-MS m/z [M+H]⁺ Calcd for C₄₂H₄₁N₆: 629.3393, Found: 629.3379.

General procedure for 2,9-bis[2-or3-(pyridinylalkylaminomethyl)phenyl]-1,10-phenanthrolines 1j-o - 2 (COOH)2

To a solution of compounds 1 (0.3 mmol) in isopropanol (11 mL) was added oxalic acid (2.4 mmol, 8 eq.). The reaction mixture was heated under reflux for 30 minutes. The precipitate was filtered, washed with isopropanol then with diethyl ether and dried under reduced pressure to give the oxalate salts of 1.

Biology

In vitro antiplasmodial activity

The *in vitro* antiplasmodial activities were tested over concentrations ranging from 39 nM to 40 μM against culture-adapted *Plasmodium falciparum* reference strains 3D7 and W2. The former strain is susceptible to chloroquine (CQ) but displays a decreased susceptibility to mefloquine (MQ); the latter is considered resistant to CQ. These two strains are obtained from the collection of the National Museum of Natural History (Paris, France). The parasites were cultivated in RPMI medium (Sig-ma-Aldrich, Lyon, France) supplemented with 0.5% Albumax I (Life Technologies Corporation, Paisley, UK), hypoxanthine (Sigma-Aldrich), and gentamicin (Sig-ma-Aldrich) with human erythrocytes and were incubated at 37 °C in a candle jar, as described previously [40]. The *P. falciparum* drug susceptibility test was carried out in 96-well flat bottom sterile plates in a final volume of 250 μL. After 48 h incubation period with the drugs, quantities of DNA in treated and control cultures of parasites in human erythrocytes were quantified using the SYBR Green I (Sigma-Aldrich) fluorescence-based method [41,42]. Briefly, after incubation, plates were frozen at -20°C until use. Plates were then thawed for 2 h at room temperature, and 100 μL of each homogenized culture was transferred to a well of a 96-well flat bottom sterile black plate (Nunc, Inc.) that contained 100 μL of the SYBR Green I lysis buffer (2xSYBR Green, 20 mM Tris base pH 7.5, 5 mM EDTA, 0.008% w/v saponin, 0.08% w/v Triton X-100). Negative controls treated with

solvent (typically DMSO or H₂O), and positive controls (CQ and MQ) were added to each set of experiments. Plates were incubated for 1 h at room temperature and then read on a fluorescence plate reader (Tecan, Austria) using excitation and emission wavelengths of 485 and 535 nm, respectively. The concentrations at which the screening drug or antimalarial is capable of inhibiting 50% of parasitic growth (IC₅₀) are calculated from a sigmoid inhibition model Emax with an estimate of IC₅₀ by non-linear regression (IC Estimator version 1.2) and are reported as means calculated from three independent experiments [43].

In vitro antileishmanial activity

L. donovani (MHOM/IN/00/DEVI) used in this study was provided by the CNR Leishmania (Montpellier, France). The effects of the tested compounds on the growth of *L. donovani* (MHOM/IN/00/DEVI) promastigotes were assessed by MTT assay [44]. Briefly, promastigotes in log-phase in Schneider's medium supplemented with 20% fetal calf serum (FCS), 2 mM L-glutamine and antibiotics (100 U/mL penicillin and 100 µg/mL streptomycin), were incubated at an average density of 106 parasites/mL in sterile 96-well plates with various concentrations of compounds previously dissolved in DMSO (final concentration less than 0.5% v/v), in duplicate. Appropriate controls treated with DMSO, pentamidine and amphotericin B (reference drugs purchased from Sigma-Aldrich) were added to each set of experiments. Duplicate assays were performed for each sample. After 72 h incubation period at 27 °C, parasite metabolic activity was determined. Each well was microscopically examined for precipitate formation. To each well was added 10 µL of 10 mg/mL MTT [3-(4,5-dimethylthiazol-2-yl)-2,5-diphenyltetrazolium bromide] solution followed by 4 h incubation time. The enzyme reaction was stopped by addition of 100 µL of 50% isopropanol/10% sodium dodecyl sulfate [45]. Plates were vigorously shaken (300 rpm) for 10 min, and the absorbance was measured at 570 nm with 630 nm as reference wavelength in a BIOTEK ELx808 Absorbance Microplate Reader (Agilent Technologies, Les Ulis, France). The IC₅₀ was defined as the concentration of drug required to inhibit by 50% of the metabolic activity of *L. donovani* promastigotes compared to the control. IC₅₀ of the parasite's growth (half maximal inhibitory concentration or IC₅₀ values) were then calculated from the obtained experimental results using a previously described regression program [43]. IC₅₀ values were calculated from three independent experiments.

In vitro antitrypanosomal activity

The effects of the tested compounds on the growth of *T. brucei brucei* were as-sessed using an Alamar Blue® assay described by Rätz, *et al.* [46] *T. brucei brucei* AnTat 1.9 (IMTA, Antwerpen, Belgium) was cultured in MEM with Earle's salts, supplemented according to the protocol of Baltz, *et al.* [47] with the following modifications: 0.5 mM mercaptoethanol (Sigma Aldrich), 1.5 mM L-cysteine (Sigma Aldrich), 0.05 mM bathocuproine sulfate (Sigma Aldrich), and 20% heat-inactivated horse serum (Gibco, France) at 37 °C and 5% CO₂. Samples were incubated at an average density of 2000 parasites/well in sterile 96-wells plates (Fisher, France) with various concentrations of compounds dissolved in 0.9% NaCl. All doses were tested in duplicate. Appropriate controls treated with solvents 0.9% NaCl or DMSO or with suramin, pentamidine, eflornithine, and fexinidazole (reference drugs purchased from Sigma Aldrich and Fluorochem, UK) were added to each set of experiments. After 69 h in-cubation period at 37 °C, 10 µL of the viability marker Alamar Blue (Fisher) was added to each well, and the plates were incubated for 5 h. The plates were read in a PerkinElmer ENSPIRE (Germany) microplate reader using an excitation wavelength of 530 nm and an emission wavelength of 590 nm. The IC₅₀ was defined as the concentration of drug necessary to inhibit by 50% the activity of *T. brucei brucei* compared to the control. IC₅₀ values were calculated using a nonlinear regression analysis of dose-response curves performed using GraphPad Prism software (GraphPad Software, San Diego, CA, USA). IC₅₀ values were calculated from three independent experiments.

Cytotoxicity evaluation

A cytotoxicity evaluation was performed using the method reported by Mosmann [44] with slight modifications to determine the cytotoxic concentrations 50% (CC₅₀) and using doxorubicin as a cytotoxic reference compound. These assays were performed in human HepG2 cells purchased from ATCC (ref HB-8065). These cells are a commonly used human hepatocarcinoma-derived cell line that has characteristics similar to those of primary hepatocytes. These cells express many hepato-cyte-specific metabolic enzymes, thus enabling the cytotoxicity of tested product metabolites to be evaluated. Briefly, cells in 100 µL of complete RPMI medium, [RPMI supplemented with 10% FCS, 1% L-glutamine (200 mM), penicillin (100 U/mL), and streptomycin (100 µg/mL)] were inoculated at 37 °C into each well of 96-well plates in a humidified chamber in 6% CO₂. After 24 h, 100 µL of medium with test compound at various

concentrations dissolved in DMSO (final concentration less than 0.5% v/v) were added, and the plates were incubated for 72 h at 37 °C. Duplicate as-says were performed for each sample. Each well was microscopically examined for precipitate formation before the medium was aspirated from the wells. After aspiration, 100 µL of MTT solution (0.5 mg/mL in medium without FCS) were then added to each well. Cells were incubated for 2 h at 37 °C. The MTT solution was removed, and DMSO (100 µL) was added to dissolve the resulting blue formazan crystals. Plates were shaken vigorously (300 rpm) for 5 min. The absorbance was measured at 570 nm with 630 nm as reference wavelength in a BIO-TEK ELx808 Absorbance Microplate Reader. DMSO was used as blank and doxorubicin (Sigma Aldrich) as positive control. Cell viability was calculated as percentage of control (cells incubated without compound). The CC_{50} was determined from the dose-response curve using the Table-Curve 2D V5.0 software (Systat Software, Palo Alto, CA, USA).

FRET melting experiments

The most antiparasitic bioactive compounds 1a-b, 1e-h have been selected for the subsequent FRET melting experiments. These were performed with dual-labeled oligonucleotides mimicking the Plasmodium telomeric sequences FPf1T [FAM-5'(GGGTTTA)3-GGG3'-TAMRA] and FPf8T [FAM-5'(GGGTTC)3GGG3'-TAMRA], the Trypanosoma 9 and 11 chromosomal sequence FTrypBT (also named FEBR1T) [FAM-5'GGGCAGGGGGTGATGGGAGGAGCCAGGG3'-TAMRA], the human telomeric sequence F21T [FAM-(GGGTTA)3-GGG3'-TAMRA] and the human duplex sequence FdxT [FAM5'-TATAGCTATA-hexaethyleneglycol-TATAGCTATA3'-TAMRA] [29,31,33,48]. The oligonucleotides were pre-folded in 10 mM lithium cacodylate buffer (pH 7.2), with 10 mM KCl and 90 mM LiCl (K^+ condition). The FAM emissions were recorded at 516 nm

using a 492-nm excitation wavelength in the absence and presence of a single compound as a function of temperature (25 to 95 °C) in 96-well microplates by using a Stratagene MX3000P real-time PCR device at a rate of 1 °C·min⁻¹. Data were normalized between 0 and 1, and the required temperature for half-denaturation of oligonucleotides corresponding to the emission value of 0.5 was taken as the T_m . Each experiment was performed in duplicate with 0.2 µM of labeled oligonucleotide and 2 µM of compound under K^+ condition. For each compound, three independent experiments were carried out.

Results and Discussion

Chemistry

The reported 2,9-bis[(pyridinylalkylaminomethyl)phenyl]-1,10-phenanthroline derivatives 1a-o were synthesized starting from the commercially available 2,9-dichloro-1,10-phenanthroline 2 (Scheme 1). The bis-[2,9-(formylphenyl)]-1,10-phenanthroline 2a-c was prepared by a direct double-Suzuki-Miyaura cross-coupling reaction of commercially available 2,9-dichloro-1,10-phenanthroline with the 2-, 3- or 4-formylphenylboronic acid performed in the presence of Pd(PPh₃)₄ as a catalyst, and in the presence of sodium carbonate as the base [25]. Reaction of various primary substituted pyridinylalkylamines with 2 gave the di-imines 3a-o, which were reduced into the 2,9-bis[(pyridinylalkylaminomethyl)phenyl]-1,10-phenanthrolines 1a-o using sodium borohydride in methanol as previously described [25]. These phenanthroline compounds 1a-o were then converted into their ammonium oxalate salts by treatment with oxalic acid in refluxing isopropanol. Table 1 summarizes the physical properties of the new synthesized 1j-o oxalates. The structure of these new substituted derivatives 1 has been confirmed by ¹H and ¹³C-NMR, and also ESI-MS analysis.

Compound		Salt ^a	mp (°C) ^b	Yield ^c %
1j	Orange crystals	2 (COOH) ₂	133-135	41
1k	Orange crystals	2 (COOH) ₂	125-127	62
1l	Beige crystals	2 (COOH) ₂	97-99	61
1m	Pale-yellow crystals	2 (COOH) ₂	99-101	77
1n	Pale-yellow crystals	2 (COOH) ₂	169-171	83
1o	Pale-yellow crystals	2 (COOH) ₂	164-166	78

^aThe stoichiometry and composition of the salts were determined by elemental analyses and obtained values were within ±0.4% of the theoretical values.

^bCrystallization solvent: 2-PrOH-H₂O.

^cThe yields only included the conversions into the ammonium oxalates.

Table 1: Physical properties of amines 1j-o.

Compound	<i>P. falciparum</i> strains IC ₅₀ values (μM) ^a		<i>L. donovani</i> IC ₅₀ values (μM) ^b	<i>Trypanosoma brucei brucei</i> IC ₅₀ values (μM) ^c	Cytotoxicity to HepG2 cells CC ₅₀ values (μM) ^d
	W2 3D7			Trypanos Antat 1.9	
CQ ^e	0.40 ± 0.04	0.11 ± 0.01	n.d. ^h	n.d. ^h	30
MQ ^e	0.016 ± 0.002	0.06 ± 0.003	n.d. ^h	n.d. ^h	n.d. ^h
Pentamidine ^f	n.d. ^h	n.d. ^h	5.5 ± 0.8	0.0002 ± 0.00006	2.3 ± 0.5
Amphotericin B ^f	n.d. ^h	n.d. ^h	0.1 ± 0.04	n.d. ^h	8.8 ± 0.6
Suramine ^g	n.d. ^h	n.d. ^h	n.d. ^h	0.03 ± 0.003	n.d. ^h
Fexinidazole ^g	n.d. ^h	n.d. ^h	n.d. ^h	0.59 ± 0.039	n.d. ^h
Eflornithine ^g	n.d. ^h	n.d. ^h	n.d. ^h	15.19 ± 0.64	n.d. ^h
Doxorubicin	n.d. ^h	n.d. ^h	n.d. ^h	n.d. ^h	0.06 ± 0.02
1a	2.56 ± 0.57	0.039 ± 0.01	2.08 ± 0.10	2.03 ± 0.14	31.66 ± 1.20
1b	16.38 ± 1.92	0.29 ± 0.07	12.07 ± 0.60	1.37 ± 0.06	11.23 ± 1.18
1c	1.51 ± 0.34	10.29 ± 2.39	> 12.5	4.13 ± 0.66	51.81 ± 5.49
1d	> 40	> 40	> 12.5	0.17 ± 0.02	2.21 ± 0.60
1e	0.15 ± 0.03	0.075 ± 0.01	> 12.5	0.17 ± 0.01	19.38 ± 2.10
1f	0.038 ± 0.01	0.075 ± 0.01	> 12.5	0.15 ± 0.01	34.67 ± 3.90
1g	0.075 ± 0.01	> 40	> 12.5	0.05 ± 0.01	3.58 ± 0.21
1h	> 40	> 40	> 12.5	0.20 ± 0.02	6.16 ± 1.35
1i	3.53 ± 0.73	2.44 ± 0.32	> 12.5	0.21 ± 0.01	30.17 ± 1.21
1j	0.84 ± 0.50	0.23 ± 0.11	> 12.5	0.51 ± 0.03	6.84 ± 0.66
1k	0.63 ± 0.12	0.097 ± 0.04	> 12.5	0.82 ± 0.03	0.10 ± 0.01
1l	0.77 ± 0.09	0.29 ± 0.08	> 12.5	1.13 ± 0.06	0.72 ± 0.04
1m	1.21 ± 0.18	10.47 ± 0.86	> 12.5	1.70 ± 0.05	61.38 ± 6.85
1n	0.25 ± 0.08	1.21 ± 0.16	> 12.5	0.88 ± 0.02	5.45 ± 0.49
1o	1.54 ± 0.31	0.15 ± 0.06	> 12.5	0.49 ± 0.05	4.80 ± 0.38

^a Values were measured against CQ-resistant and MQ-sensitive strain W2 and the CQ-sensitive and MQ-resistant strain 3D7.

^b IC₅₀ values were measured against the promastigotes of *Leishmania donovani* strain. The IC₅₀ (μM) values correspond to the means +/- standard deviations from 3 independent experiments.

^c IC₅₀ values were measured against the slender bloodstream trypomastigotes of *Trypanosoma brucei brucei* AnTat 1.9 strain. The IC₅₀ (μM) values correspond to the means +/- standard deviations from 3 independent experiments with each concentration tested in duplicate in all experiments.

^d CC₅₀ values were measured against HepG2 cells. The CC₅₀ (μM) values correspond to the means +/- standard deviations from 3 independent experiments.

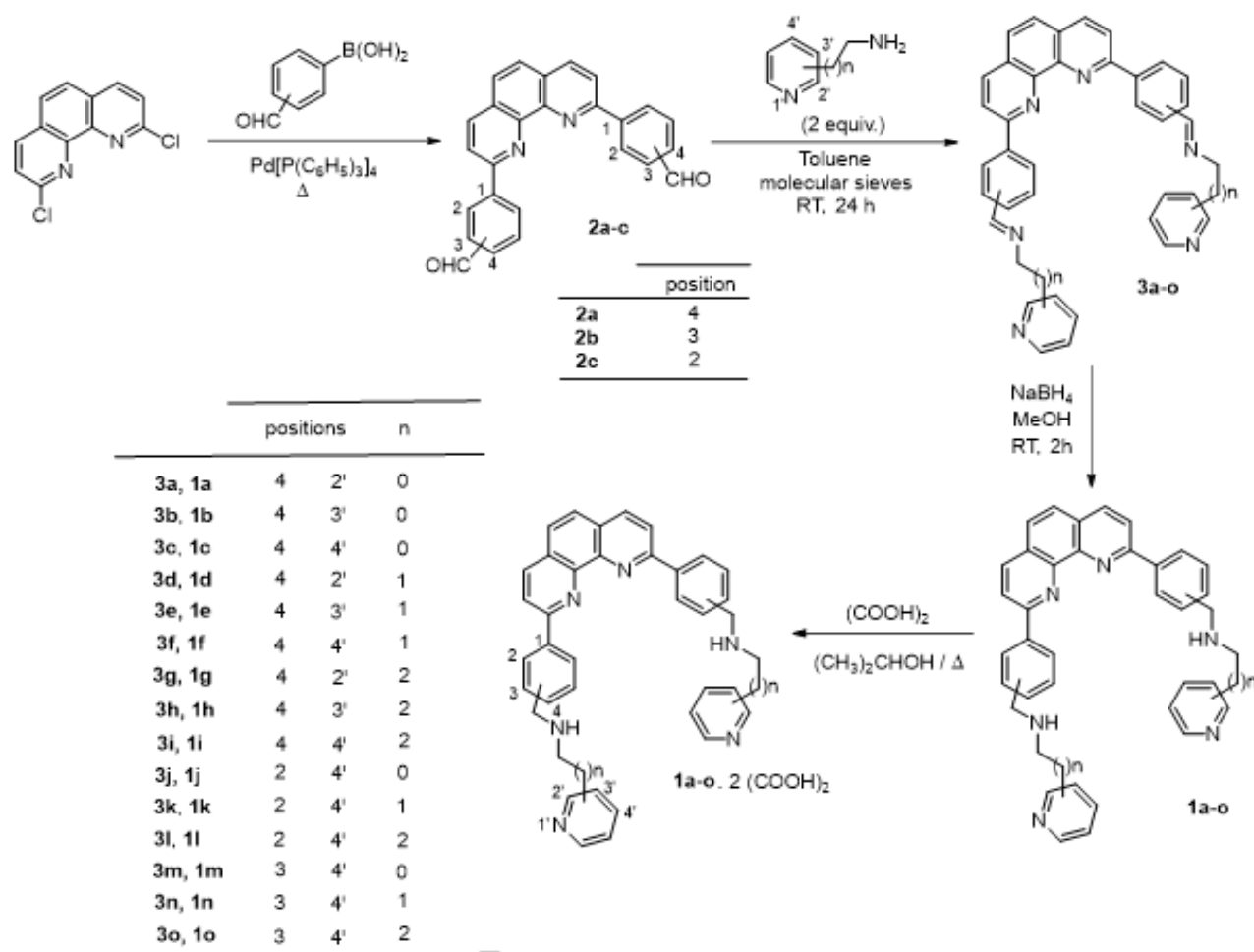
^e CQ and MQ were used as antiplasmodial compounds of reference.

^f Pentamidine and amphotericin B were used as antileishmanial compounds of reference.

^g Suramine, pentamidine, fexinidazole and eflornithine were used as antitrypanosomal compounds of reference.

^h n.d.: not done.

Table 2: *In vitro* sensitivity of *P. falciparum*, *L. donovani* and *T. brucei brucei* strains to compounds 1a-o and cytotoxicity of these compounds in HepG2 cells.



Scheme 1: General procedure for the preparation of new phenanthroline compounds 1a-o.

Biological evaluation

In vitro antimalarial activity

Against the *P. falciparum* CQ-resistant strain W2, compound 1f pyridin-4-ylethylaminomethyl side chains at position 4 of the benzyl rings was found to be the most active with an IC_{50} of 0.038 μM . In comparison, its counterparts with pyridin-2-ylethylaminomethyl or pyridin-3-ylethylaminomethyl groups at position 4 (compounds 1d and 1e) were significantly less active ($IC_{50} > 40 \mu\text{M}$ for 1d; $IC_{50} = 0.15 \mu\text{M}$ for 1e) than phenanthroline 1f. In the sub-series 1a-c, in which the derivatives were substituted by pyridinylmethylaminomethyl chains at position 4, compound

1c with the pyridin-4-yl substitution was found the most active against the W2 strain with an IC_{50} 1.51 μM in comparison with the pyridin-2-yl and pyridin-3-yl substituted phenanthrolines 1a-b ($IC_{50} = 2.56$ and 16.38 μM , respectively). In contrast, for pyridinylpropylaminomethyl substitution at position 4, the phenanthroline 1g with a pyridin-2-yl moiety was noticed more active than its pyridin-3-yl and pyridin-4-yl homologues 1h-i; $IC_{50} = 0.075 \mu\text{M}$ for 1g versus > 40 and 3.53 μM for 1h and 1i. For compounds 1j-l substituted by pyridin-4-ylalkylaminomethyl chains at position 2 of the benzyl rings, no significant differences in the antiparasitic bioactivity against the W2 strains was observed; IC_{50} were found ranging from 0.63 to 0.84 μM .

Against the 3D7 strain, the 2,9-bis[(pyridinylalkylaminomethyl)phenyl]-1,10-phenanthroline derivatives 1a, 1e-f were found the most active compounds with IC_{50} of 0.039 and 0.075 μM , respectively. Moreover, compounds 1f and 1i bearing pyridin-4-ylalkylaminomethyl side chains at position 4 of the benzyl rings displayed better activity than their analogues substituted with pyridin-3-ylalkylaminomethyl or pyridin-2-ylalkylaminomethyl side chains (IC_{50} = 0.075 and 2.44 μM , respectively for these bioactive derivatives), with the exception of compound 1c which showed less good antimalarial activity (IC_{50} = 10.29 μM). In addition, the substitution of the pyridin-4-ylalkylaminomethyl side chains at position 2 or 3 of the benzyl nucleus in these phenanthroline series was not found detrimental in comparison with the substitution in position 4 against this 3D7 *P. falciparum* strains (IC_{50} ranging from 0.097 to 1.21 μM for compounds 1j-l and 1n-o). However, derivative 1m was found less active than its other homologues (IC_{50} = 10.47 μM). In term of structure-activity relationships, it was quite difficult to draw conclusions about the different substitutions on the benzyl moiety, the length of the alkyl chain and the position of the pyridine ring substitution. In addition, the 1,10-phenanthrolines 1e and 1k which were disubstituted with a C_2 pyridin-4-yl chain in position 2 and 4 of the benzyl rings, exhibited a better biological activity than their C_1 or C_3 homologues, compounds 1c, 1i, 1j and 1l, respectively; i.e. IC_{50} of 0.075-0.097 μM for 1e and 1k versus 0.23-10.29 μM for 1c, 1i, 1j and 1l. For a substitution of the alkylpyridin-4-yl chain in position 3 of the benzyl, compound 1o with a propylpyridin-4-yl chain (IC_{50} = 0.15 μM) was noticed more active than derivatives with an ethyl or methyl chain (phenanthrolines 1m-n).

In vitro antileishmanial activity against promastigote forms

In order to better understand the biological profile of our new phenanthrolines 1, some complementary antiparasitic analyses were also performed. Notably, *P. falciparum* belongs to the coccidian protozoan parasite family. Therefore, *in vitro* activity against flagellate protozoan parasite *L. donovani* was evaluated (Table 2). The reference drugs amphotericin B and pentamidine had IC_{50} values of 0.10 μM and 5.50 μM , respectively, against *L. donovani*. Only the phenanthroline 1a was found active against the promastigote forms of *L. donovani* with an IC_{50} of 2.08 μM . In addition, compound 1b displayed a moderate activity against *L. donovani* (IC_{50} = 12.07 μM).

In vitro activity against Trypanosoma brucei brucei

These newly synthesized phenanthrolines 1a-o were then evaluated against *T. brucei brucei*. Pentamidine, suramine, fexinidazole, and eflornithine were also used here as reference compounds. The screening data are presented in Table 2. All phenanthrolines 1a-o were active against *T. brucei brucei* with IC_{50} values ranging from 0.05 to 4.13 μM ; and most of them showed an antiparasitic activity around the μM value. The best efficacy against the *T. brucei brucei* strain was observed with compound 1g with an IC_{50} of 0.05 μM , the same order of magnitude as the reference drug suramine (IC_{50} = 0.03 μM).

Cytotoxicity and selectivity index

In order to assess selectivity of action, the cytotoxicities of these new synthesized antiparasitic phenanthroline compounds 1 were evaluated *in vitro* in the human cell line HepG2, which is a commonly used human-derived hepatocarcinoma cell line, and express many hepatocyte-specific metabolic enzymes. The aim of this assay was to evaluate the impact of metabolic activation of the tested compounds on cell viability. The cytotoxic concentrations 50% (CC_{50}) were determined, and selectivity indexes (SI), defined as the ratios of cytotoxic to antiparasitic activities ($SI = CC_{50}/IC_{50}$) were calculated. The results of cytotoxicity assays and the associated SI values are presented in Table 3. Most of these new phenanthrolines 1 that were found active against the various parasites showed significant cytotoxicity against the HepG2 cells with CC_{50} values ranging from 0.10 to 61.38 μM . Concerning the W2 strain, the calculated SIs were noticed between 0.06 and 912.4. For the CQ sensitive strain 3D7, the SIs were found from 0.06 to 811.8. Analyses of these SI values led us to identify the phenanthrolines 1e and 1f as very interesting compounds with SI of 129.2 and 912.4 for the CQ resistant strain W2 strain, and compounds 1a and 1f with SI of 811.8 and 462.3 for the 3D7 strain, respectively. Against the *T. brucei brucei* strain, three phenanthrolines 1e-1f and 1i showed SI of 114.0, 231.1 and 143.7, respectively. These promising SI values could indicate that these new nitrogen heterocyclic compounds warrant further investigations into their potential use as antiparasitic drugs.

FRET-melting experiments

As the telomeres of the parasites *P. falciparum* and *Trypanosoma* could be potential targets of this kind of heterocyclic derivatives,

Compound	Selectivity Index ^a			
	HepG2/W2	HepG2/3D7	HepG2/ <i>L. donovani</i>	HepG2/ <i>Tryp.</i>
CQ	75	272	n.d. ^b	n.d. ^b
Pentamidine	n.d. ^b	n.d. ^b	0.42	11500
Amphotericin B	n.d. ^b	n.d. ^b	88.0	n.d. ^b
1a	12.4	811.8	15.2	15.6
1b	0.69	38.72	0.93	8.20
1c	34.31	5.03	n.d. ^b	12.54
1d	<0.06	< 0.06	n.d. ^b	13.0
1e	129.2	258.4	n.d. ^b	114.0
1f	912.37	462.27	n.d. ^b	231.13
1g	47.73	<0.09	n.d. ^b	71.6
1h	<0.15	<0.15	n.d. ^b	30.8
1i	8.55	12.36	n.d. ^b	143.67
1j	8.14	29.74	n.d. ^b	13.41
1k	0.16	1.03	n.d. ^b	0.12
1l	0.94	2.48	n.d. ^b	0.64
1m	50.73	5.86	n.d. ^b	36.11
1n	21.8	4.50	n.d. ^b	6.19
1o	3.12	32.0	n.d. ^b	9.79

^aSI was defined as the ratio between the CC₅₀ value on the HepG2 cells and the IC₅₀ value against the *P. falciparum* W2 or 3D7 or *Trypanosoma brucei brucei* strains.

^b n.d.: not done.

Table 3: Selectivity indexes of compounds 1a-o.

we have also investigated the stabilization of the *P. falciparum* telomeric or *T. brucei brucei* chromosomal G-quadruplexes by our best bioactive antiparasitic compounds 1a and 1e-g through a FRET melting assays. We used a FRET melting assay to determine the degree to which the new phenanthroline derivatives stabilize the G-quadruplexes formed by oligonucleotides with *P. falciparum* or *T. brucei brucei* as well as human telomeric sequences. For this purpose, we used two fluorescently labeled *P. falciparum* telomeric and one *T. brucei brucei* chromosomal sequences (FPf1T, FPf8T and FtrypBT) and one human telomeric sequence (F21T).

To probe the G4 selectivity of our selected ligands 1a and 1e-g over duplex DNA, a FRET melting assay was performed using a duplex control sequence, FdxT. For comparison, we evaluated reference G4 ligand PhenDC3 and the antimalarial reference drugs

CQ and MQ. To enable comparison of selectivities, we calculated the difference (DTm) between the Tm of the G-quadruplex formed by FPf1T, FPf8T, FtrypBT (FEBR1T), F21T or FdxT in the presence or absence of each selected compound. These DTm values are presented in table 4. For these selected compounds 1a and 1e-g, the DTm values ranged from 4.9 to 17.0 °C at 2 μM ligand concentration.

The stabilization of our compounds was also investigated against the fluorescently labelled human telomeric sequence F21T. To probe the G4 selectivity of our heterocyclic ligands 1 over duplex DNA, a FRET melting assay was performed using a duplex control sequence, FdxT.

The best ligand which stabilize all the four G-quadruplexes sequences was compound 1g (Table 4). Indeed, the best di-nitrogen

Compound	DT _m (°C) ^a		DT _m (°C) ^a		DT _m (°C) ^a		DT _m (°C) ^a		DT _m (°C) ^a	
	FPf1T		FPf8T		FtrypBT		F21T		FdxT	
PhenDC3	24.6	± 0.1	24.7	± 0.2	19.2	± 0.2	26.3	± 0.1	0.1	± 0.2
CQ	1.9	± 0.1	2.4	± 1.2	n.d. ^b		2.4	± 1.1	n.d. ^b	
MQ	3.1	± 0.5	6.6	± 2.3	n.d. ^b		2.6	± 0.5	n.d. ^b	
1a	5.9	± 1.6	6.6	± 0.9	4.9	± 0.2	7.7	± 1.1	-1.3	± 0.1
1e	8.0	± 1.3	9.0	± 1.1	5.1	± 0.6	5.9	± 1.2	-0.9	± 0.2
1f	8.6	± 0.5	9.7	± 0.6	5.3	± 0.4	8.3	± 1.0	-1.2	± 0.1
1g	13.6	± 0.8	14.3	± 0.6	9.0	± 0.2	17.0	± 0.2	0.2	± 0.1

^aDT_m of FPf1T, FPf8T, FtrypBT, F21T and FdxT (0.2 μM) were recorded in 10 mM lithium cacodylate (pH 7.2), 10 mM KCl, 90mM LiCl. PhenDC3 was tested at 0.5 μM, whereas CQ and MF at 1μM. Error margins correspond to SD of three replicates.

^bn.d.: not determined.

Table 4: FRET-melting values for the selected compounds 1a and 1e-g with FPf1T, FPf8T, FtrypBT, F21T and FdxT in K⁺ conditions at 2 μM.

heterocyclic ligand which stabilize all the three parasitic (FPf1T, FPf8T, FtrypBT) and the human F21T G-quadruplexes sequences was the 2,9-bis[4-(pyridin-2-ylpropylaminomethyl)phenyl]-1,10-phenanthroline 1g with DT_m values ranging from 9.0 to 17.0 °C. The other selected compounds 1a and 1e-f exhibited moderate stabilization profile for all the G4 forming sequences. Among the tested compounds, derivatives 1a and 1e-g displayed a better stabilization profile for both the *P. falciparum* telomeric sequences than the *T. brucei brucei* chromosomal G-quadruplex.

From a general point of view, all our ligands 1a and 1e-g were found to show lower stabilization than the reference PhenDC3 ligand. FRET assays showed there was no binding to duplex DNA sequence.

Conclusion

In the present report, we described the design, the synthesis, the antiprotozoal activities, and the *in vitro* cytotoxicity toward human cells of a novel series of 2,9-bis[(pyridinylalkylamino methyl)phenyl]-1,10-phenanthroline derivatives. These new “quinoline-like” derivatives were tested for their *in vitro* antiparasitic activity toward the CQ-sensitive 3D7 and CQ-resistant W2 *P. falciparum* strains, the promastigote form of *L. donovani*, and a *T. brucei brucei* strain. Among these new synthesized nitrogen heterocyclic molecules, a few of them were identified as potential *in vitro* antiplasmodial leads with IC₅₀ ranging from 0.038 to 2.56, and 0.039 to 1.21 mM on the W2 and 3D7 strains of *P. falciparum*, respectively. The 2,9-bis[(pyridinylalkylaminomethyl)phenyl]-1,10-phenanthroline 1f was identified as the most potent antimalarial candidate with a ratio of cytotoxic to antiparasitic activities of 912.4 against the *P. falciparum* CQ-resistant strain W2. In addition, we also identified phenanthrolines 1a and 1f with indexes of selectivity of 811.8 and 462.3, respectively for the CQ-sensitive strain 3D7.

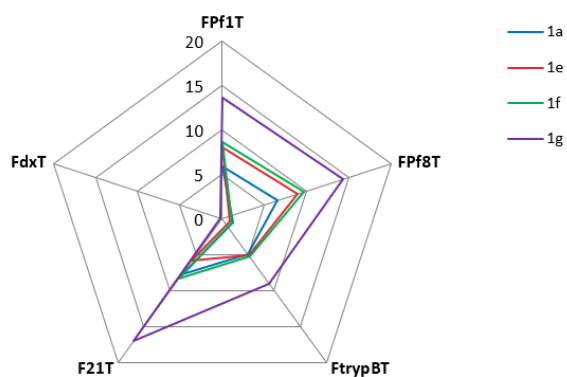


Figure 2: Stabilization specificity profile of 1a and 1e-g (2 μM) toward various G4 oligonucleotides. The difference in T_m in presence and absence of 1a and 1e-g; ΔT_m, in °C is plotted for each sequence. 4 quadruplexes and one duplex (FdxT) were tested.

Unfortunately, only one of our compounds (phenanthroline 1a) showed activity against the promastigote forms of *L. donovani*. Moreover, the antiprotozoal activity spectrum of our new synthesized derivatives using a *T. brucei brucei* strain revealed IC_{50} values ranging from 0.05 to 4.13 μ M, which warrant further investigations. The 2,4-bis[(substituted-aminomethyl)phenyl]quinazoline 1f was also identified as the most potent trypanosomal candidate with selectivity index (SI) of 231.1 on *Trypanosoma brucei brucei* strain. In addition, the *in vitro* cytotoxicity of these new heterocyclic compounds was assessed on the human HepG2 cell line. Structure-activity relationships of these new synthetic compounds are here also discussed, as well as their relative ability of targeting *P. falciparum* or *Trypanosoma* telomeres as an hypothetical mechanism of action. Thus, as the telomeres of the parasites could constitute interesting targets, we have also investigated the possibility of targeting *Plasmodium* telomeres or *Trypanosoma* chromosomes by stabilizing the *Plasmodium* or *Trypanosoma* G-quadruplexes sequences through FRET melting assays with our best bioactive compounds. However, we found no convincing correlations between the antiparasitic activity and selectivity of these derivatives and their binding to G-quadruplexes. These derivatives are therefore unlikely to be specifically cytotoxic via G-quadruplex binding. Moreover, it would be now interesting to enlarge the pharmacological evaluation of these new phenanthrolines derivatives 1 by studying their mechanism of action through further investigations such as the inhibition of beta-hematin formation or of the apicoplast functions. Finally, the new substituted 2,9-bis[(pyridinylalkylaminomethyl)phenyl]-1,10-phenanthrolines could open the way to new valuable medicinal chemistry scaffolding in the antiprotozoal domain.

Conflict of Interest

The authors report no conflicts of interest. The authors alone are responsible for the content and writing of the paper.

Acknowledgments

The authors would like to thank Pr. Philippe Grellier, department RDDM at Muséum National d'Histoire Naturelle (Paris, France), for providing generously the 3D7 and W2 *P. falciparum* strains.

Bibliography

1. World malaria report (2022).
2. WHO Guidelines for malaria (2022).
3. Webinar: Launch of new antimalarial drug resistance strategy for Africa (2022).
4. Global Malaria Programme: Tools for monitoring antimalarial drug efficacy (2022).
5. Belete TM. "Recent progress in the development of new antimalarial drugs with novel targets". *Drug Design, Development and Therapy* 14 (2020): 3875-3889.
6. Kim J., et al. "Structure and drug resistance of the *Plasmodium falciparum* transporter PfCRT". *Nature* 576 (2019): 315-320.
7. Alibert-Franco S., et al. "Efflux Mechanism, an Attractive Target to Combat Multidrug Resistant *Plasmodium falciparum* and *Pseudomonas aeruginosa*". *Current Medicinal Chemistry* 16 (2009): 301-317.
8. Baird JK. "8-Aminoquinoline Therapy for Latent Malaria". *Clinical Microbiology Reviews* 32 (2019): e00011-19.
9. Dola VR., et al. "Synthesis and Evaluation of Chirally Defined Side Chain Variants of 7-Chloro-4-Aminoquinoline To Overcome Drug Resistance in Malaria Chemotherapy". *Antimicrobial Agents and Chemotherapy* 61 (2017): e01152-16.
10. Manohar S., et al. "4-Aminoquinoline based molecular hybrids as antimalarials: an overview". *Current Topics in Medicinal Chemistry* 14 (2014): 1706-1733.
11. O'Neill PM., et al. "A medicinal chemistry perspective on 4-aminoquinoline antimalarial drugs". *Current Topics in Medicinal Chemistry* 6 (2006): 479-507.
12. Krogstad DJ., et al. "Efflux of chloroquine from *Plasmodium falciparum*: mechanism of chloroquine resistance". *Science* 238 (1987): 1283-1285.
13. Fidock DA., et al. "Mutations in the *P. falciparum* digestive vacuole transmembrane protein PfCRT and evidence for their role in chloroquine resistance". *Molecular Cell* 6 (2000): 861-871.
14. Roepe PD. "Molecular and physiologic basis of quinoline drug resistance in *Plasmodium falciparum* malaria". *Future Microbiology* 4 (2009): 441-455.

15. Deshpande S., *et al.* "4-aminoquinolines: An Overview of Antimalarial Chemotherapy". *Medicinal Chemistry* 6 (2016): 1.
16. Kumar S., *et al.* "Recent advances in novel heterocyclic scaffolds for the treatment of drug-resistant malaria". *Journal of Enzyme Inhibition and Medicinal Chemistry* 31 (2016): 173-186.
17. Van de Walle T., *et al.* "Recent contributions of quinolines to antimalarial and anticancer drug discovery research". *European Journal of Medicinal Chemistry* 226 (2021): 113865.
18. Douglas B., *et al.* "Attempts to find new antimalarials. Part XXVIII. *p*-Phenanthroline derivatives substituted in the 4-position". *Journal of the Chemical Society* (1949): 1017-1022.
19. Yapi AD., *et al.* "In Vitro and in Vivo Antimalarial Activity of Derivatives of 1,10-Phenanthroline Framework". *Archiv der Pharmazie - Chemistry in Life Sciences* 339 (2006): 201-206.
20. Sall C., *et al.* "Design, synthesis, and biological activities of conformationally restricted analogs of primaquine with a 1,10-phenanthroline framework". *Bioorganic and Medicinal Chemistry Letters* 18 (2008): 4666-4669.
21. Wijayanti MA., *et al.* "Additive in vitro antiplasmodial effect of *N*-alkyl and *N*-benzyl-1,10-phenanthroline derivatives and cysteine protease inhibitor e64". *Malaria Research and Treatment* 2010 (2010): 540786.
22. Sholikhah EN., *et al.* "In vitro antiplasmodial activity and cytotoxicity of newly synthesized *N*-alkyl and *N*-benzyl-1,10-phenanthroline derivatives". *Southeast Asian Journal of Tropical Medicine and Public Health* 37 (2006): 1072-1077.
23. Zuma AA., *et al.* "In vitro study of the trypanocidal activity of anilinophenanthrolines against *Trypanosoma cruzi*". *Parasitology International* 83 (2021): 102338.
24. Ending the neglect to attain the sustainable development goals: a road map for neglected tropical diseases 2021-2030.
25. Fernandez-Prada C., *et al.* "Repurposed molecules: A new hope in tackling neglected infectious diseases". In *In Silico Drug Design: Repurposing Techniques and Methodologies*. 1st ed.; Roy, K. Ed.; Elsevier: Amsterdam, (2019): 119-160.
26. Guillon J., *et al.* "Design, synthesis, and antiproliferative effect of 2,9-bis[4-(pyridinylalkylaminomethyl)phenyl]-1,10-phenanthroline derivatives on human leukemic cells by targeting G-quadruplex". *Archiv der Pharmazie (Weinheim)* 354 (2021): e2000450.
27. Guillon J., *et al.* "Synthesis, antimalarial activity, and molecular modeling of new pyrrolo[1,2-*a*]quinoxalines, bispyrrolo[1,2-*a*]quinoxalines, bispyrido[3,2-*e*]pyrrolo[1,2-*a*]pyrazines, and bispyrrolo[1,2-*a*]thieno[3,2-*e*]pyrazines". *Journal of Medicinal Chemistry* 47 (2004): 1997-2009.
28. Dassonville-Klimpt A., *et al.* "Absolute Configuration and Antimalarial Activity of erythro-Mefloquine Enantiomers". *ChemPlusChem* 78 (2013): 642-646.
29. Guillon J., *et al.* "Design, synthesis and antimalarial activity of novel bis{*N*-[(pyrrolo[1,2-*a*]quinoxalin-4-yl)benzyl]-3-aminopropyl}amine derivatives". *Journal of Enzyme Inhibition and Medicinal Chemistry* 32 (2017): 547-563.
30. Jonet A., *et al.* "Synthesis and Antimalarial Activity of New Enantiopure Aminoalcoholpyrrolo[1,2-*a*]quinoxalines". *Medicinal Chemistry* 14 (2018): 293-303.
31. Guillon J., *et al.* "Design, synthesis, and antiprotozoal evaluation of new 2,4-bis[(substituted-aminomethyl)phenyl]quinoline, 1,3-bis[(substituted-aminomethyl)phenyl]isoquinoline and 2,4-bis[(substituted-aminomethyl)phenyl]quinazoline derivatives". *Journal of Enzyme Inhibition and Medicinal Chemistry* 35 (2020): 432-459.
32. Dassonville-Klimpt A., *et al.* "Design, synthesis, and characterization of novel aminoalcohol quinolines with strong in vitro antimalarial activity". *European Journal of Medicinal Chemistry* 228 (2022): 113981.
33. Guillon J., *et al.* "Design, synthesis, and antiprotozoal evaluation of new 2,9-bis[(substituted-aminomethyl)phenyl]-1,10-phenanthroline derivatives". *Chemical Biology and Drug Design* 91 (2018): 974-995.
34. Calvo EP., *et al.* "G-Quadruplex ligands: Potent inhibitors of telomerase activity and cell proliferation in *Plasmodium falciparum*". *Molecular and Biochemical Parasitology* 207 (2016): 33-38.
35. Tidwell RR., *et al.* "Dicationic compounds which selectively recognize G-quadruplex DNA". EP 1792613A2 (2007).
36. Leeder WM., *et al.* "Multiple G-quartet structures in pre-edited mRNAs suggest evolutionary driving force for RNA editing in trypanosomes". *Scientific Reports* 6 (2016): 29810.
37. Lombrana R., *et al.* "Transcriptionally Driven DNA Replication Program of the Human Parasite *Leishmania major*". *Cell Reports* 16 (2016): 1774-1786.

38. Bottius E., *et al.* "Plasmodium falciparum Telomerase: De Novo Telomere Addition to Telomeric and Nontelomeric Sequences and Role in Chromosome Healing". *Molecular and Cellular Biology* 18 (1998): 919-925.
39. Raj DK., *et al.* "Identification of telomerase activity in gametocytes of Plasmodium falciparum". *Biochemical and Biophysical Research Communications* 309 (2003): 685-688.
40. Desjardins RE., *et al.* "Quantitative assessment of antimalarial activity *in vitro* by a semiautomated microdilution technique". *Antimicrobial Agents and Chemotherapy* 16 (1979): 710-718.
41. Bennett TN., *et al.* "Novel, Rapid, and Inexpensive Cell-Based Quantification of Antimalarial Drug Efficacy". *Antimicrobial Agents and Chemotherapy* 48 (2004): 1807-1810.
42. Bacon DJ., *et al.* "Comparison of a SYBR Green I-Based Assay with a Histidine-Rich Protein II Enzyme-Linked Immunosorbent Assay for *In Vitro* Antimalarial Drug Efficacy Testing and Application to Clinical Isolates". *Antimicrobial Agents and Chemotherapy* 51 (2007): 1172-1178.
43. Kaddouri H., *et al.* "Assessment of the Drug Susceptibility of Plasmodium falciparum Clinical Isolates from Africa by Using a Plasmodium Lactate Dehydrogenase Immunodetection Assay and an Inhibitory Maximum Effect Model for Precise Measurement of the 50-Percent Inhibitory Concentration". *Antimicrobial Agents and Chemotherapy* 50 (2006): 3343-3349.
44. Mosmann T. "Rapid colorimetric assay for cellular growth and survival: application to proliferation and cytotoxicity assays". *Journal of Immunological Methods* 65 (1983): 55-63.
45. Emami SA., *et al.* "Inhibitory Activity of Eleven Artemisia Species from Iran against Leishmania Major Parasites". *Iranian Journal of Basic Medical Sciences* 15 (2012): 807-811.
46. Rüz B., *et al.* "The Alamar Blue assay to determine drug sensitivity of African trypanosomes (*T.b. rhodesiense* and *T.b. gambiense*) *in vitro*". *Acta Tropica* 68 (1997): 139-147.
47. Baltz T., *et al.* "Cultivation in a semi-defined medium of animal infective forms of Trypanosoma brucei, T. equiperdum, T. evansi, T. rhodesiense and T. gambiense". *EMBO Journal* 4 (1985): 1273-1277.
48. De Cian A., *et al.* "Fluorescence-based melting assays for studying quadruplex ligands". *Methods* 42 (2007): 183-195.